PRAMANA © Indian Academy of Sciences Vol. 68, No. 3
— journal of March 2007
physics pp. 529–534

Core temperature in super-Gaussian pumped air-clad photonic crystal fiber lasers compared with double-clad fiber lasers

P ELAHI[1], H NADGARAN[2] and F KALANTARIFARD[3]
[1]Department of Physics, Payame Noor University, Shiraz, Iran
[2]Department of Physics, College of Science, Shiraz University, Shiraz, Iran
[3]Qeshm Azad University, Qeshm, Iran
E-mail: pelahi@spnu.ac.ir; nadgaran@susc.ac.ir

MS received 29 May 2006; revised 30 September 2006; accepted 18 October 2006

Abstract. In this paper we investigate the core temperature of air-clad photonic crystal fiber (PCF) lasers pumped by a super-Gaussian (SG) source of order four. The results are compared with conventional double-clad fiber (DCF) lasers pumped by the same super-Gaussian and by top-hat pump profiles.

Keywords. Photonics crystal fiber lasers; super-Gaussian pump source; double-clad fiber lasers.

PACS No. 42.55.Wd

1. Introduction

High power rare-earth-doped fiber lasers have recently attracted considerable attention due to their high efficiency and high beam quality compared to traditional gas and solid-state lasers [1–5]. A new class of fiber lasers, called photonic crystal fiber (PCF) lasers, has come up [6,7] with some properties superior to conventional fiber lasers. Among those superiorities, one can name a shift of zero-dispersion wavelength towards the visible spectral range and their operations as a single-mode fiber over a large wavelength range. The gain medium of such fiber lasers can be fabricated by doping rare-earth ions into their core. By surrounding the inner cladding with a web of silica bridges, the double-clad concept can be transferred to such fibers. In power scaling studies of high power fiber lasers, the role of thermo-optic effects acquire much attention because standard fiber laser design will eventually lead to high core temperature when dealing with high power regimes [8]. Limpert *et al* [9] investigated thermo-optic effects in air-clad photonic crystal fiber lasers. Their work, however, assumes a uniform deposition of heat power density into the fiber.

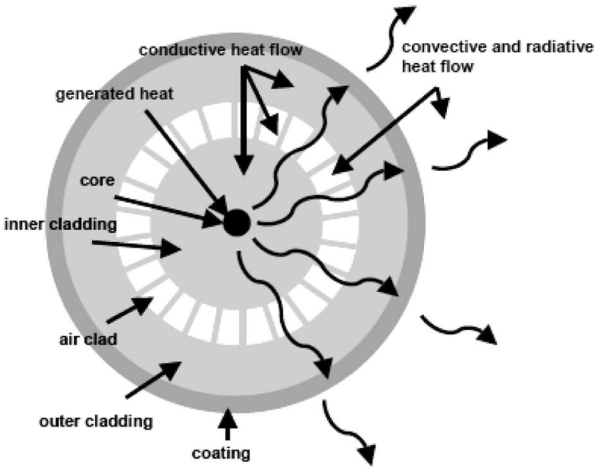

Figure 1. Heat flow in air-clad photonic crystal fiber lasers [9].

In this paper, we calculate the core temperature of PCF and DCF lasers and compare their thermal behavior under super-Gaussian and top-hat pump profiles [10].

2. Theory of heat transfer

Suppose the fiber core is irradiated by a super-Gaussian beam profile of order four. Due to quantum defect between the pump and the laser photons, heat is generated in the fiber core and so the power of heat deposition per unit volume is given by [10]

$$Q(r) = Q_0 \exp\left(\frac{-r^4}{w_0^4}\right), \tag{1}$$

where w_0 is the spot size of the pump source. The governing heat equation in steady state is written as

$$\vec{\nabla} \cdot \vec{q}'' = Q(r), \tag{2}$$

where $\vec{q}''$ is the heat flux. The heat generated in the core region is transferred to the surface of the fiber by thermal conduction through fused silica and the coating material. The heat flux is related to the temperature distribution function, T as

$$\vec{q}'' = -k\,\vec{\nabla} T, \tag{3}$$

where k is the thermal conductivity of fused silica.

These processes are illustrated in figure 1.

The temperature distribution inside the fiber is determined by considering conductive heat flow in the fused silica and convective and radiative heat flow in the air-clad and heat removal from coatings to the ambient region. At steady state, the sum of the input rate of heat flow ($\dot{q}_{\rm in}$) at a certain surface should be equal to the output one ($\dot{q}_{\rm out}$). So

$$\sum \dot{q}_{\rm in} = \sum \dot{q}_{\rm out} \tag{4}$$

and $(\dot{q}/A) = q''$ where A denotes the area of the surface of the fiber. The heat flow in the form of radiation from the surface A is given by Stefan–Boltzmann law as

$$\dot{q}_{\rm rad} = \sigma\,\varepsilon\,A(T_{\rm s}^4 - T_{\rm sur}^4), \tag{5}$$

where $\sigma = 5.6705 \times 10^{-8}\,{\rm W/(m^2\,K^4)}$ is the Stefan–Boltzmann constant, ε is the emission factor, $T_{\rm s}$ and $T_{\rm sur}$ are the surface and surrounding temperatures, respectively.

The convective heat flow from the surface A is given by

$$\dot{q}_{\rm conv} = h\,A(T_{\rm s} - T_\infty), \tag{6}$$

where T_∞ is the ambient air temperature and h is the convective heat transfer coefficient which for a cylinder of diameter d can be approximately given by [9]

$$h = \bar{c}\left(\frac{T_{\rm s} - T_\infty}{d}\right)^{1/4}, \tag{7}$$

where $\bar{c} = 1.3\ {\rm W/(m^{1.75}\,K^{1.25})}$ is the temperature-dependent coefficient for convective cooling for air [9].

The radial heat flow from the surface A in a medium with thermal conductivity k is given by

$$\dot{q}_{\rm cond} = k\,A\,\frac{\Delta T}{\Delta r}, \tag{8}$$

where Δr is the path of the heat flow and ΔT is the temperature difference along Δr.

The conductive heat flow in the silica bridges can be calculated as

$$\dot{q}_{\rm cond} = k \times \text{No. of bridges} \times \text{Bridge width} \times L\frac{\Delta T}{\text{Bridge length}}, \tag{9}$$

where No. of bridges × Bridge width shows the silica bridge area and L is the fiber length.

3. Numerical results

By using the above considerations, the core temperature of the fiber in both PCF and DCF lasers were calculated numerically. In our calculations we used a Yb-doped fiber laser with the following specifications:

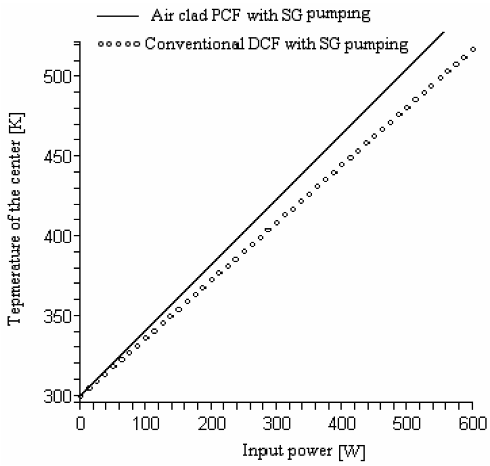

Figure 2. Temperature of the center of DCF laser compared to PCF laser as a function of input power.

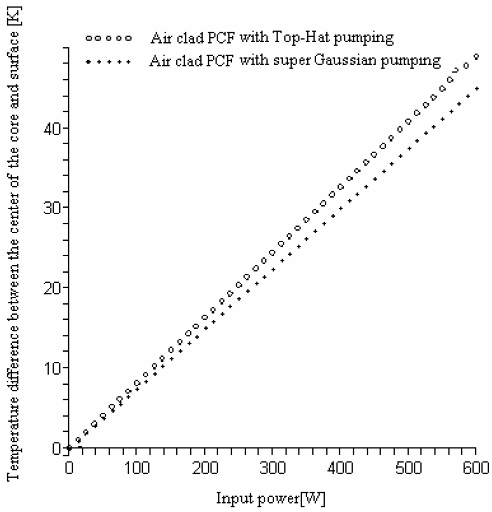

Figure 3. Temperature difference between the center of the core and the surface of the PCF laser for both top-hat and super-Gaussian pumping.

Fiber length=5 m
Core diameter=28 μm
First clad diameter=150 μm
Second clad diameter= 440 μm
Bridge width=0.4 μm
Bridge length=50 μm
Number of bridges = 42
Thickness of coating=20 μm
The pump and lasing wavelengths are 0.915 μm and 1.120 μm, respectively.

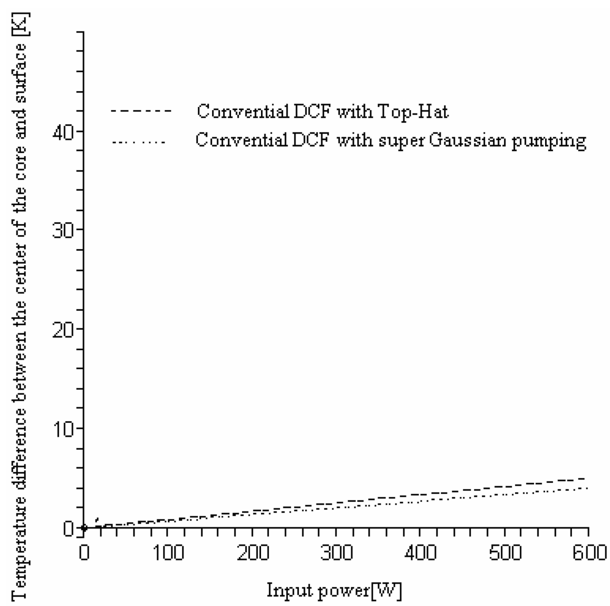

Figure 4. Temperature difference between the center of the core and the surface of the DCF laser for both top-hat and super-Gaussian pumping.

Figure 2 compares the temperature of the center of the PCF laser pumped by a super-Gaussian profile as a function of input power with the conventional DCF laser under the same pump [10]. As seen from the figure, the temperature of the center of DCF laser is less than that of the PCF laser. A 50 μm beam spot size was assumed in this case. In both cases the fiber is cooled by air and its convective heat transfer coefficient was assumed to be $h = 1 \times 10^{-3}$ W/(cm^2 K). The ambient air temperature T_∞ was assumed to be 300 K and the thermal conductivity was taken as $k = 1.38 \times 10^{-2}$ W(cm-K)$^{-1}$.

Figure 3 shows the temperature difference between the center of the core and the surface of the laser as a function of input power for PCF laser under both top-hat and super-Gaussian pump profiles. The figure clearly shows a reduction of the temperature difference when PCF laser is pumped by super-Gaussian source [10]. In figure 4 the same plots are given for DCF laser under top-hat and super-Gaussian pumps. Here the temperature difference is much lower compared to PCF laser of figure 3.

4. Conclusion

This paper is mainly concerned with the temperature behavior of PCF and DCF lasers. As the results show, the PCF core temperature is higher than that of DCF when both are pumped by a super-Gaussian pump profile. This result reveals the superiority of DCF laser over PCF one, despite the fact that their core temperature is close to each other. The most important results of figures 3 and 4 are two-fold.

First, the super-Gaussian pump brings less temperature difference for both PCF and DCF lasers causing lower temperature gradient across the laser core and less thermo-optics effects.

Secondly, the temperature difference is very much lower in the case of DCF for both top-hat and super-Gaussian profiles. Therefore, if one is to decide about a PCF or DCF laser in the high power regime, the optimum choice might be a DCF laser with a super-Gaussian pump.

References

[1] J Limpert, A Lien, H Zelmer and A Tunnerman, *Electron. Lett.* **39(8)**, 645 (2003)
[2] A Galvanauskas, *IEEE J. Sel. Top. Quantum Electron* **7**, 504 (2001)
[3] Y Jeong, J K Sahu, D N Payne and J Nilsson, *Optics Express* **12**, 6088 (2004)
[4] Y Jeong, J K Sahu, R P Williams, D J Richardson, K Fuurusawa and J Nilsson, *Electron. Lett.* **39**, 977 (2003)
[5] Y Jeong, J K Sahu, S Baek, C Alegria, D B S Soh, C Codemard and J Nilsson, *Opt. Commun.* **234**, 315 (2004)
[6] J C Knight, T A Birks, P St J Russell and D M Atkin, *Opt. Lett.* **21**, 1547 (1996)
[7] J Limpert, T Scheribler, S Notle, H Zellmer, T Tunnermann, R Ilieve, F Ledere, J Broeng, G Vienne, A Peterson and C Jacobsen, *Optics Express* **11**, 818 (2003)
[8] David C Brown and Hanna J Hoffman, *IEEE J. Quantum Electron.* **37**, 207 (2001)
[9] J Limbert, T Schreiber, A Liem, S Nolte, H Zellmer, T Peschel, V Guyenot and A Tunnermann, *Optics Express* **11**, 2982 (2003)
[10] H Nadgaran and P Elahi, *Pramana – J. Phys.* **65**, 95 (2005)